

Mechanics Based Design of Structures and Machines



An International Journal

ISSN: 1539-7734 (Print) 1539-7742 (Online) Journal homepage: www.tandfonline.com/journals/lmbd20

Lambda-shaped hangers: an innovative fatigue-resistant hanger system for pedestrian suspension bridges

Arman Khatar, Salar Farahmand-Tabar & Majid Barghian

To cite this article: Arman Khatar, Salar Farahmand-Tabar & Majid Barghian (2025) Lambda-shaped hangers: an innovative fatigue-resistant hanger system for pedestrian suspension bridges, Mechanics Based Design of Structures and Machines, 53:10, 7172-7191, DOI: 10.1080/15397734.2025.2499901

To link to this article: https://doi.org/10.1080/15397734.2025.2499901







Lambda-shaped hangers: an innovative fatigue-resistant hanger system for pedestrian suspension bridges

Arman Khatar (D), Salar Farahmand-Tabar (D), and Majid Barghian (D)

Department of Structural Engineering, Faculty of Civil Engineering, University of Tabriz, Tabriz, Iran

ABSTRACT

Susceptibility to dynamic loads is a critical concern for lightweight and slender suspension footbridges, especially those with limited damping capabilities. The performance of these structures can be influenced by the type of the hanger system. Suspension bridge hangers are generally configured as either vertical or inclined. While inclined hangers offer enhanced aerodynamic stability, they are more vulnerable to fatigue and may exhibit distress or slackness due to their configuration. In this paper, a lambdashaped hanger system is proposed to mitigate the internal forces, reduce slackness, and enhance fatigue resistance. The general behavior of the system is investigated, and the impact of key variables on its performance is analyzed, comparing it against vertical and inclined hanger systems. Results indicate that the lambda-shaped hanger system significantly enhances the behavior of the bridge in most cases compared to vertical or inclined hangers. The lambda-shaped hanger configuration demonstrates favorable fatigue performance, with a 44.2% force increment, closely matching the 44% increment of vertical hangers and outperforming inclined hangers by 3.9%. This suggests the lambda-shaped configuration's superior fatigue resistance. When the bridge is subjected to the most critical live load pattern, the maximum force distribution occurs in the inclined hanger system. In contrast, the lambda-shaped hangers exhibit a lower force distribution by 34.1% than the case with the inclined hanger system.

ARTICLE HISTORY

Received 5 August 2024 Accepted 24 April 2025

KEYWORDS

suspension bridge; vertical hangers; inclined hangers; Lambda-shaped hangers; slackness; Fatique

1. Introduction

Dynamic loads pose a significant risk to flexible suspension footbridges, especially those with slender structures that can lead to oscillation issues (Dey, Narasimhan, and Walbridge 2021; Otavio et al. 2022). These footbridges are highly susceptible to wind and vibrations caused by pedestrian activities, such as walking, jumping, and running. When the crowd intensity surpasses a critical threshold, dynamic responses in the footbridge and discomfort for pedestrians become apparent (Lievens et al. 2018; Wang et al. 2021). The trend of constructing lightweight footbridges has grown in recent years, but this increased flexibility can lead to larger vibration amplitudes under dynamic forces. Traditionally, footbridges were designed to withstand static loads only, but modern footbridges must consider vibration phenomena due to their slenderness. However, adhering to natural frequency requirements specified in codes (AASHTO GSDPB-2-II1 2015; BS5400 1978; DIN-Fachbericht 102 2009; ENV 1995-22 2005; Fib Bulletin 32 32 2005) can be challenging for very slender and lightweight structures like stress ribbon and suspension bridges.

To understand the dynamic response of footbridges, factors such as natural frequencies, bridge mass, damping properties, and pedestrian loading are crucial (Avci 2016; Carpineto, Lacarbonara, and Vestroni 2010; García-Diéguez et al. 2021). If the vibration behavior fails to meet comfort criteria, adjustments in the design or the incorporation of damping devices might be necessary. Lightweight suspension footbridges have lower natural frequencies, making them more susceptible to resonance (Li, Xie, and Au 2022; Zhou and Wan 2022). Vibrations caused by pedestrians further exacerbate the serviceability problems of suspension footbridges (Al-Smadi et al. 2022; Dey, Narasimhan, and Walbridge 2018; Nyawako and Reynolds 2018; Saber, Samani, and Pellicano 2023). Cable systems, such as main cables and hangers, are used to increase the stiffness of suspension bridges and improve the vibration characteristics. Inclined hangers, acting as damping elements against dynamic loads, are more effective than vertical hangers. However, inclined hangers are prone to fatigue, slackness under excessive tension, and early wear compared to vertical hangers. The mentioned issues require modification to achieve an optimum system (Farahmand-Tabar and Barghian 2020a, 2020b).

The number of slacked hangers relies on dynamic load types (Farahmand and Shirgir 2025; Farahmand-Tabar and Barghian 2019, 2021; 2023; Shirgir, Farahmand-Tabar, and Aghabeigi 2024). Pedestrian traffic, density, and comfort needs significantly affect suspension footbridge dynamics. Heavy traffic may strain hangers, causing unwanted vibrations. To address this, adjustments can be made, such as limiting structural vibrations, stiffening, and reducing internal forces. The Millennium Bridge in London experienced significant swaying due to pedestrian movement (Dallard et al. 2001; Newland 2003; Pavic et al. 2002), leading to its temporary closure. Similar issues were observed in the steel footbridge in Forchheim, Germany (Seiler, Fischer, and Huber 2002). Studies by Kerr and Bishop (2001) on vertical forces during walking indicated a comfortable pace between 1.7 and 2.2 Hz. Figueiredo et al. (2008) introduced a load model considering pedestrian movement's impact on footbridge dynamics. Nakamura (2003) found that pedestrians excite various vibration modes. The Mindaugas highway arch bridge faced high crowd loading, which was improved by adding inclined suspenders. Wu, Takahashi, and Nakamura (2001, 2003) studied the effects of slackened cables on bridge vibrations. Melchor et al. (2004) examined pedestrian suspension bridges with S-shaped inclined hangers.

Several studies highlighted issues with inclined hangers in bridges like the Humber Bridge and Severn Bridge in England and the Bosphorus Bridge in Turkey (Al-Khalili 1984; Suh and Change 2000). Pellegrino, Cupani, and Modena (2010) explored hanger arrangements to reduce fatigue stress. Bachmann (2002) proposed acceleration limits for footbridges. Huang, Thambiratnam, and Perera (2005) investigated vibration characteristics in cable-supported bridges. Studničková (2004) assessed pedestrian load effects on footbridge dynamics. Brownjohn (2005) and Lai, Gentile, and Mulas (2017) researched footbridge vibration serviceability. Finite element analysis was used to study footbridge dynamics, notably the Millennium Bridge (Hauksson 2005; Zivanovic 2008). Zivanovic (2008) and Zivanovic et al. (2005) reviewed footbridge vibration serviceability. Bassoli, Gambarelli, and Vincenzi (2018) described a footbridge model and testing. Wang et al. (2019) studied a footbridge in Portugal prone to pedestrian-induced vibrations, aiming to establish a control system.

In this study, a novel hanger system is introduced to improve the dynamic properties (Faravelli and Ubertini 2009, 2009) of inclined hanger systems in a suspension footbridge and address the disadvantages as mentioned earlier. The new arrangement, which is introduced as the lambda-shaped hanger system, is proposed to control the dynamic responses of the bridge by reducing the slackness/overstressing problem that exists in inclined hangers and avoiding the related fatigue phenomenon (Gao, Wang, and Ma 2022; Lepidi, Gattulli, and Vestroni 2009; Mei, Jin, and Sun 2018; Pothula et al. 2012; Zhu et al. 2019). The new arrangement uses the vertical and inclined arrangement together to use the advantages of each system simultaneously. Therefore, the performance of all systems is compared to each other to show the capability of the new system.

2. Hanger systems

2.1. Vertical and inclined hanger systems

As a conventional type of hanger system, a vertical hanger model is considered subjected to vertical and horizontal load (Figure 1). Considering the assumed boundary condition, the system will not slack. Inclined hangers are another type of hanger system that is modeled and subjected to vertical and horizontal loads (Figure 1). By applying a lateral load to the inclined hanger system, one hanger is over-stressed and another hanger is slacked. This will cause fatigue due to repeated loading and unloading cycles in hangers. The load–displacement and axial force diagram are illustrated in Figure 1.

Inclined hangers are characterized by the fact that each hanger can become either slack or overstressed under heavy loads. This distress arises from the relative longitudinal movement between the main cable and the suspended deck, which induces a change in stress in the two parts of adjacent hangers (Figure 2). Slackness occurs when the compression induced by live loading exceeds the dead load tension initially built into the hangers. The extent of stress variation depends on the included angle between two adjacent hangers, which is determined during construction and adjusted at various points of attachment to the cable to protect the hangers from overstress and slack conditions under extreme live loads. However, the difference in vertical

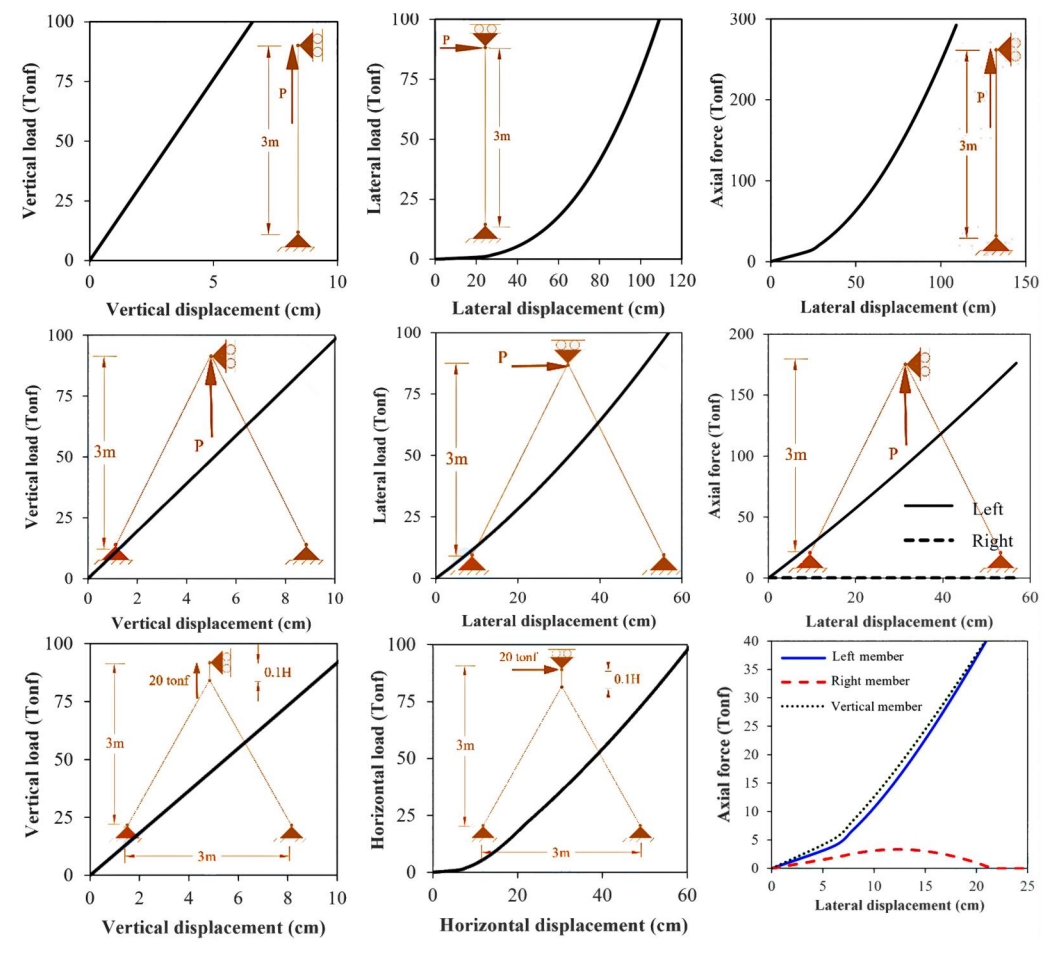


Figure 1. Load-displacement diagram for different hanger systems.

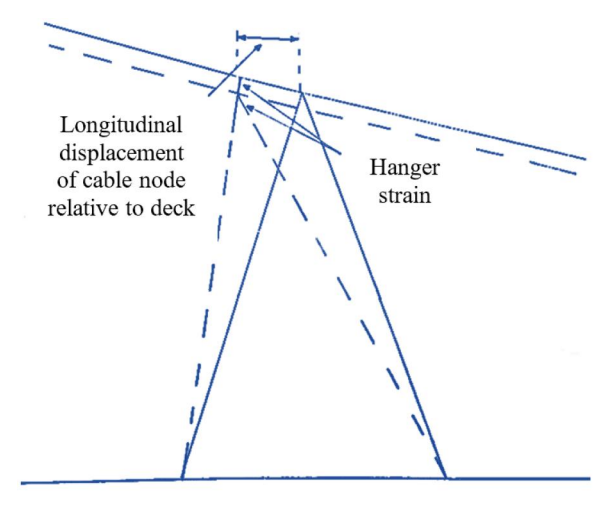


Figure 2. Hanger strain due to bridge oscillations.

loads causes continuous fluctuation in the stress levels of the hangers. These fluctuations—where axial tension in the hanger alternates with compression—can lead to rupturing due to fatigue. This type of fatigue has been considered in the present research. By introducing a lambda-shaped hanger, the weakness of conventional inclined hangers is mitigated. The proposed hanger remains in tension and avoids slackness, thereby preventing fatigue failure.

2.2. The proposed lambda-shaped hanger system

Beside the conventional system of hangers, the lambda-shaped hanger model is shown in Figure 3. The maximum amount of lateral stiffness is achieved when the ratio of vertical member length to the total height of the hanger is less than 10%. However, applied lateral force is transferred to each inclined hanger unproportioned. Considering this case, it seems that this type of hanger system is also vulnerable to fatigue. However, this system refrains from fatigue due to its applied constraint for being in hanger slackness. In other words, dislike inclined hangers, no hanger experiences slackness during lateral loading, and both hangers are under tension. The load-displacement diagram for a lambda-shaped hanger is shown in Figure 1. In lambda-shaped hangers, a low lateral force results in low stiffness, whereas increasing the applied load leads to a corresponding increase in stiffness. Figure 3—which illustrates the desired configuration—can be easily constructed. A comparable configuration is often seen in suspension bridges with inclined hangers. The primary distinction lies in the connecting component: instead of a cylindrical element, a square flat plate is employed, with a rod member positioned atop the plate to create the arrangement shown in Figure 3. It is important to note that the hangers are pre-tensioned; therefore, this structural configuration does not present any practical or mechanical issues.

3. Analysis of the bridge models

3.1. Bridge model

The considered Soti Ghat Bridge Figure 4a is a pedestrian suspension bridge in Nepal. The height of the bridge tower measures 16 m. The conventional hangers were considered and substituted with lambda-shaped ones (Figure 4b and c) within the analyzed model. This alteration aimed to investigate how the different hanger systems impact the performance of the footbridge when subjected to pedestrian loads. All three bridges had an equal number of hangers, each with the same

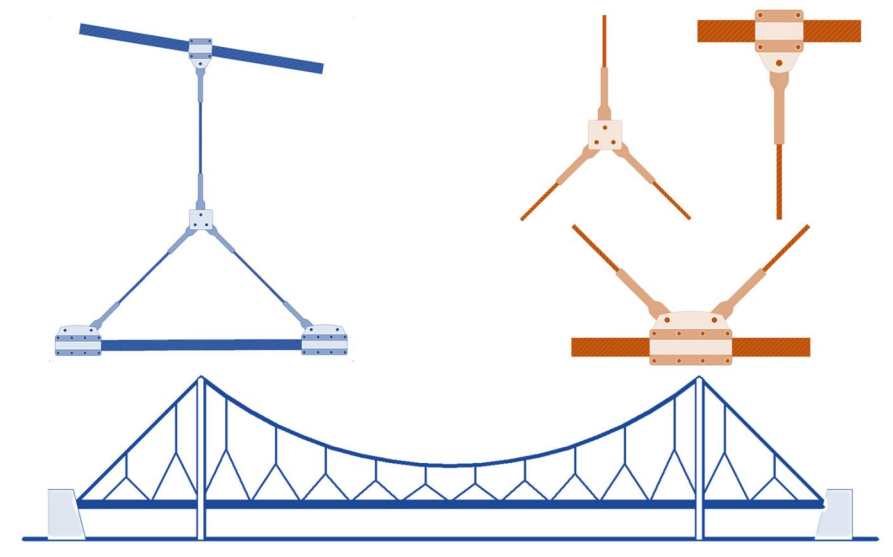


Figure 3. Lambda-shaped hanger system: configuration and cable fittings.

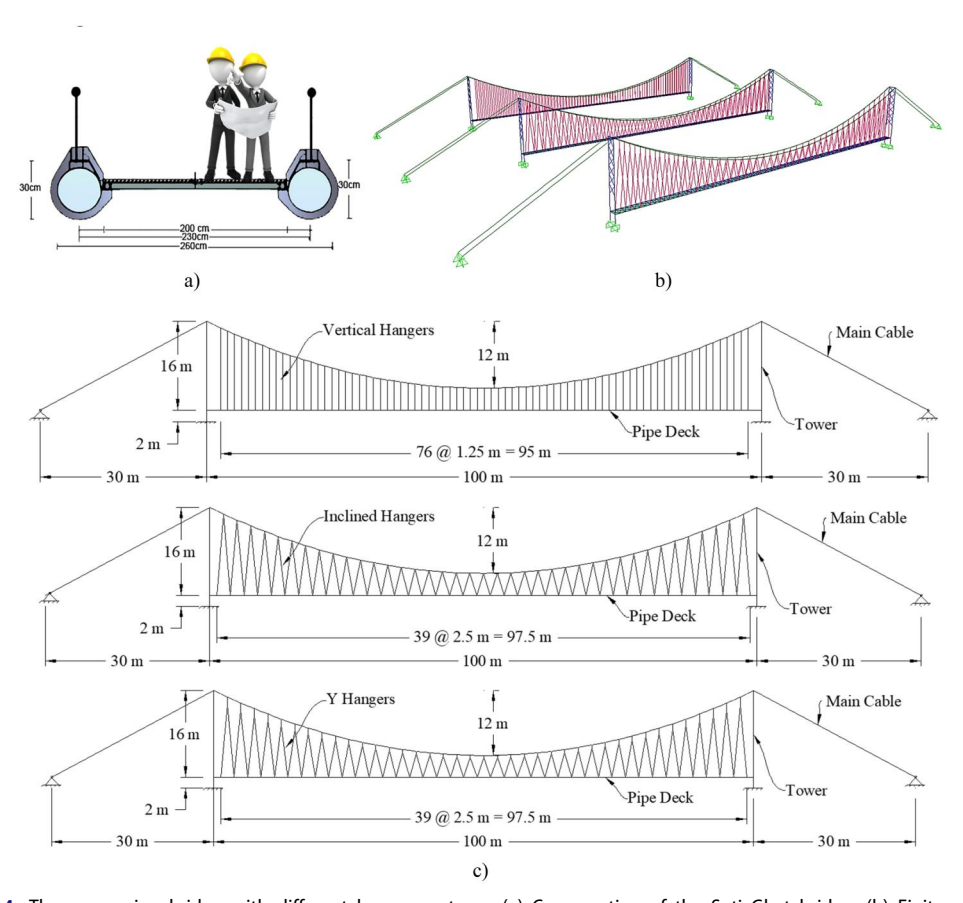


Figure 4. The suspension bridge with different hanger systems. (a) Cross-section of the Soti Ghat bridge. (b) Finite element models. (c) Hanger systems.

cross-section diameter. The span length is 100 m, while the load-bearing deck is set at a width of 2 m. To enhance the structural integrity of the span, two longitudinal beams with a height of 0.3 m were incorporated. The main cables exhibited a sag of 12 meters, with diameters measuring 120 mm, and the hangers were 26 mm in diameter.

Transverse beams, forming pinned connections between the longitudinal beams, were situated at 125 cm intervals. The deck was additionally reinforced with lateral horizontal braces. The connection between the deck and the main cables was achieved through hangers spaced at 2.5 meters in bridges featuring inclined and lambda-shaped hangers. In comparison, bridges employing vertical hangers had intervals of 1.25 m, coinciding with the placement of crossbeams. The bridge towers were constructed using steel pipes, stabilized by diagonal lateral braces. In the simulation, all structural members were represented using steel material properties, including Young's modulus of 2×10^{11} N/m² and a weight density of 7.85×10^4 N/m³. The main cables and hangers were assigned the following material properties: a yield stress (f_{ν}) of 1.18×10^9 N/m², and an ultimate strength (f_u) of 1.57 × 10⁹ N/m².

The pre-stressed load of the cables was determined based on cable weight, sag, and axial stiffness. It was assumed that each mode shared identical damping ratios. Given that the footbridge is constructed from steel, a damping ratio of 0.004 has been adopted for the structure. The deck components were modeled as shell elements with end releases, designed to mimic simple support conditions by employing pin connections to the supporting beams. The longitudinal beams were modeled using 3D beam elements, as were the steel pipe towers. To capture the flexible behavior of the cables, each cable element was divided into 40 segments.

3.2. Load cases

Pedestrian suspension bridges commonly face a variety of loads over time, stemming from pedestrians, bicycles, motorcycles, animals, and external factors such as temperature effects (Liu et al. 2024), earthquakes, and wind. In this study, the bridge was subjected to both static dead loads and live loads. The live load was applied symmetrically and asymmetrically as a distributed load with a magnitude denoted as "q" according to Eq. (1) (Barghian and Faridani 2011).

$$q = \left(2 + \frac{150}{L + 150}\right) \frac{kN}{m^2}; 2 < q < 3 \tag{1}$$

In Equation (1), L represents the loaded length in meters, and q stands for the load intensity in kN/m². The specifics of the load quantities and distribution patterns are presented in Table 1. The dead load of the bridge was computed using software to account for gravity-related forces. The value of the pre-stressed load in the cables was determined by considering factors such as cable weight, sag, and axial stiffness. The analysis will illustrate that the most critical scenarios for live loads arose from the symmetric configuration labeled as A and the asymmetric pattern designated as D.

3.3. Analysis

The primary purpose of the study is to improve the behavior of hangers and reduce slackness. First, the suspension bridge with vertical and inclined hangers was analyzed for dead and live loads to discuss the force distribution in hangers and other bridge members. Then, the hangers were replaced with lambda-shaped hangers within a similar condition. Then, all stages of loading on the bridge were applied. The structural analysis of the bridge was conducted considering the geometric nonlinearity and large deformations, consistently with modeling methodologies employed for all hanger configurations of the case study bridge. The SAP2000 software package

Table 1. Applied load patterns due to pedestrian live loads.

Load pattern	Loaded length (m)	Intensity of gravity loads (kN/m²)	Load pattern name
A	100	2.6	
В	100	2.6	
С	100	2.6	
D	50	2.75	
E	50	2.75	

was utilized to perform the numerical simulations (as illustrated in Figure 4b) and solve the analytical models.

4. Results and discussions

4.1. Parametric analysis to reach the optimal lambda-shaped hanger system

The lambda-shaped hanger was chosen with a cable diameter of 1 cm, the hanger height of 3 m (H=3), and a span of 3 m (L=3). The ratio of vertical member length to the total height of the hanger (α) was chosen to be 0.1. To evaluate the lateral performance of the system, a horizontal load of 20 tons (P=20) was applied to the hanger system. The system was analyzed statically, and geometric nonlinearity with large deformations was considered. The load–displacement diagram for the lambda-shaped hanger system is shown in Figure 1. For low lateral load values, the stiffness is very low, while the lateral stiffness of the hanger system is increased when the slope is increased. Therefore, the lambda-shaped hanger system has a hardening behavior. Also, the axial forces of the lambda-shaped hanger elements are shown in Figure 1. In this system, the applied load has caused tension in all cables. This is the advantage of the proposed system. By increasing the lateral displacement, the tensile force in the right-hand side member decreases after passing a maximum peak. As the lateral displacement increases further after a downtrend, the tensile force in the right-hand side member gradually decreases and approaches zero, causing the member to become slack.

4.1.1. Prestressing effect

Due to the nonlinear behavior of cables, applying the prestressing to cables increases their stiffness. The pre-stress effect on the lambda-shaped hanger system is given in Figure 5a. Three pre-stressing loads—minimal force, 5 tons, and 20 tons—were applied, along with varying lateral loads (*P*). By applying prestressing load, the diagram slope increases; therefore, the stiffness is increased. The effect of prestressing load on the slacking of the right-hand side member is shown in Figure 5a. By increasing the prestressing load, the slacking of the member is delayed.

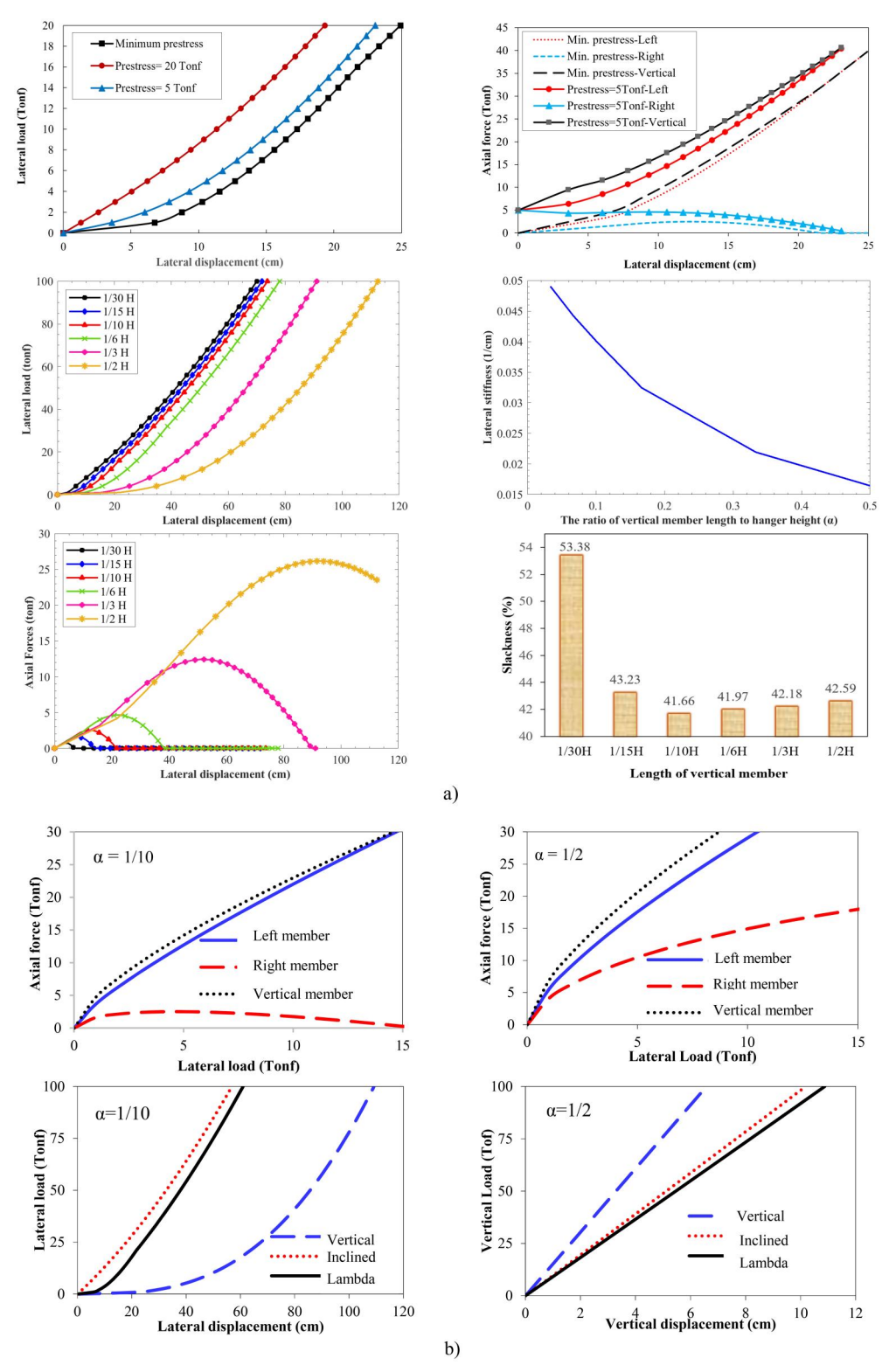


Figure 5. Parametric analysis results to reach the optimal lambda-shaped hanger system. (a) Effects of prestress and length of the vertical members. (b) Performance of the vertical, inclined and lambda-shaped hangers.

4.1.2. Length effect of the vertical member

The hangers connect the main cable to the deck. Hangers' intervals are usually fixed from each other, and only the heights of the hangers are changed. The change in the length of the vertical member in the lambda-shaped hangers alters the performance of the system. Therefore, the geometric characteristics of the system should be selected in such a way that by changing the length of the vertical member, the system's performance should not change. The length ratio of the vertical member to the full hanger is discussed as an influential variable in the lambda-shaped hanger system. A load–displacement diagram for the lambda-shaped hanger system with various lengths of the vertical member is shown in Figure 5a. As shown, reducing the length of vertical members increases the lateral stiffness of the entire hanger system. The effect of length variation in the vertical member of the lambda-shaped hanger versus the corresponding lateral stiffness is also given in Figure 5a. The increase in the length of the vertical member reduces the lateral stiffness of the lambda-shaped hanger system.

4.1.3. Slackness of cables

Lateral load on inclined hangers causes cable slackness. Loading and unloading cycles lead to slackness in some cables and excessive tension in others, creating fatigue. In lambda-shaped hangers, one of the inclined members may slack under large lateral loads, but applying prestressing force resolves this issue. The length of the vertical member also affects slackness. Figure 5a shows that increasing the vertical member length delays slackness in inclined members. The ratio of displacements at maximum axial forces to those at slacking force was determined for inclined members of lambda-shaped hangers, indicating strength participation. Reducing the vertical member length increases hanger system slackness. Figure 5a also shows slackness percentages for inclined members with various vertical member lengths under lateral load. The most slackness occurs with the shortest vertical member. The lambda-shaped hanger system with $\alpha=0.1$ has the least slackness among the investigated systems.

4.1.4. Force distribution among members

The axial force of the vertical member (for $\alpha=1/10$ and $\alpha=0.5$) is shown in Figure 5b. For $\alpha=1/10$, the highest force was generated in the vertical member. Forces in the left cable (LC) and right cable (RC) were 11% and 82% less than the force in the vertical member, respectively. The force distribution between the members in the system with $\alpha=0.5$ is better than the system with $\alpha=0.1$. The highest axial force belonged to the vertical member. The force in LC is around 15%, and the force in RC is about 50% less than the achieved force in the vertical member. Applying the lateral load to hangers with $\alpha>0.1$ in the lambda-shaped hanger arrangement enhances the force distribution between its inclined members. However, by increasing the amount of α to more than 0.1, the lateral stiffness of the hanger system is reduced.

4.1.5. Cross-section of hangers in different systems

The cross-sections of the vertical, inclined, and lambda hangers considering the same steel quantity were compared. For this reason, a one-story frame consisting of three members of 3 m was considered. The frame was used considering different hanger systems: vertical, inclined, and lambda hangers with $\alpha=1/30$, 1/15, 1/10, 1/6, 1/3, and 1/2. The amount of consumed steel for the inclined hanger was calculated as a base item. For other arrangements, the cable length used for any arrangement was calculated. Based on the inclined hanger, other systems' volumes were kept constant, and their lengths and cross-sections were calculated for the mentioned volume. The result is shown in Table 2. It is seen that the smallest cross-section is related to the inclined system, while the lambda-shaped hanger, with α equals 1/15, is placed second.

Table 2. Cable cross sections for different hangers with equal amounts of seen.						
Cable length (cm)	Cross section (cm ²)					
300.00	2.24					
670.90	1.00					
574.31	1.17					
600.04	1.12					
633.15	1.06					
647.81	1.04					
655.37	1.02					
653.01	1.03					
	Cable length (cm) 300.00 670.90 574.31 600.04 633.15 647.81 655.37					

Table 2. Cable cross-sections for different hangers with equal amounts of steel.

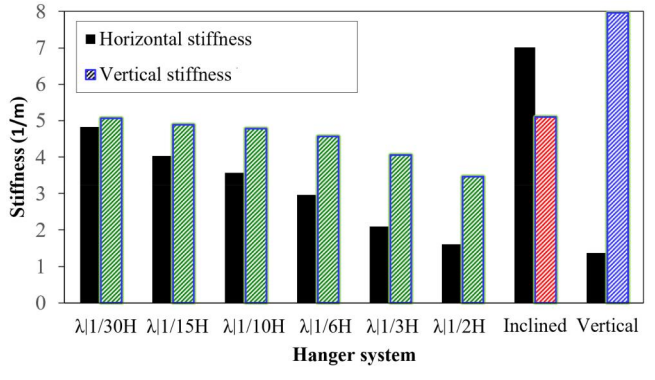


Figure 6. Comparing the stiffness of vertical, inclined, and lambda-shaped hangers.

4.1.6. Comparing the performance of hangers

The load-displacement diagram for vertical, inclined, and lambda-shaped hanger systems is shown in Figure 5b. Load applied to the inclined hanger, causing the graph to be a straight line. But at the beginning of the loading process on the vertical hanger, a huge displacement is created, and after the initial displacement (nonlinear behavior), the graph becomes almost a line. The behavior of the lambda-shaped hanger at the beginning of loading is the same as that of the vertical hanger. However, with increasing load, the behavior of this system begins to resemble that of the inclined hangers. Figure 5b also presents the load-displacement diagram under vertical load for vertical, inclined, and lambda-shaped hangers. Under vertical loads, the graph for all three systems becomes linear.

4.1.7. Stiffness of the hanger systems

Given that all systems contain the same amount of steel, a comparison of hanger stiffness becomes meaningful. Figure 6 compares the horizontal and vertical stiffness of hanger systems. Cable cross-sections are shown in Table 2. Vertical hangers have the lowest horizontal stiffness, 80.5% less than inclined hangers. Lambda-shaped hangers have higher horizontal stiffness than vertical but lower than inclined hangers. The horizontal stiffness of lambda-shaped hangers with the α value equal to 1/30, 1/15, 1/10, 1/6, 1/3, and 1/2 is obtained 31%, 42.5%, 49%, 58%, 70%, and 77% lower than inclined hangers, respectively. Reducing vertical member length increases horizontal stiffness. For $\alpha = 1/10$, the lambda-shaped hanger's horizontal stiffness is 49% lower than inclined hangers and 62% higher than vertical hangers. Figure 6 shows that the vertical hangers have the highest vertical stiffness, while inclined hangers are 30.3% lower. Reducing vertical member length in lambda-shaped hangers increases vertical stiffness. With $\alpha = 1/30$, 1/15, 1/10, 1/6, 1/3, and 1/2, vertical stiffness is 36%, 38%, 40%, 43%, 49%, and 57% lower than vertical hangers, respectively. For $\alpha = 1/10$, lambda-shaped hangers have 40% lower vertical stiffness than vertical hangers and 6% lower than inclined hangers. The best system should consider these

variables. Inclined hangers increase horizontal stiffness but cause slackness and fatigue due to force fluctuation. Lambda-shaped hangers reduce slackness and provide good lateral stiffness. With α =1/10, lambda-shaped hangers minimize slackness and resolve fatigue issues in inclined hangers.

4.2. The performance of hanger systems on the bridge

The load is applied along the bridge span. Under load pattern A, hangers do not slack or overstress. This study identifies the critical loading pattern for suspension bridges with vertical, inclined, and lambda hangers. Figure 7a shows force distribution in vertical and inclined hangers due to various loadings, with an average force of 4.19 and 4.23 kN, respectively. The maximum force under dead load in vertical hangers is 8.28 kN, while it ranges from 0.16 to 8.69 kN in inclined ones. Also, Figure 7a shows force distribution in the lambda-shaped hangers. The average force in the upper section of lambda-shaped hangers (8.5 kN) is approximately 50% higher

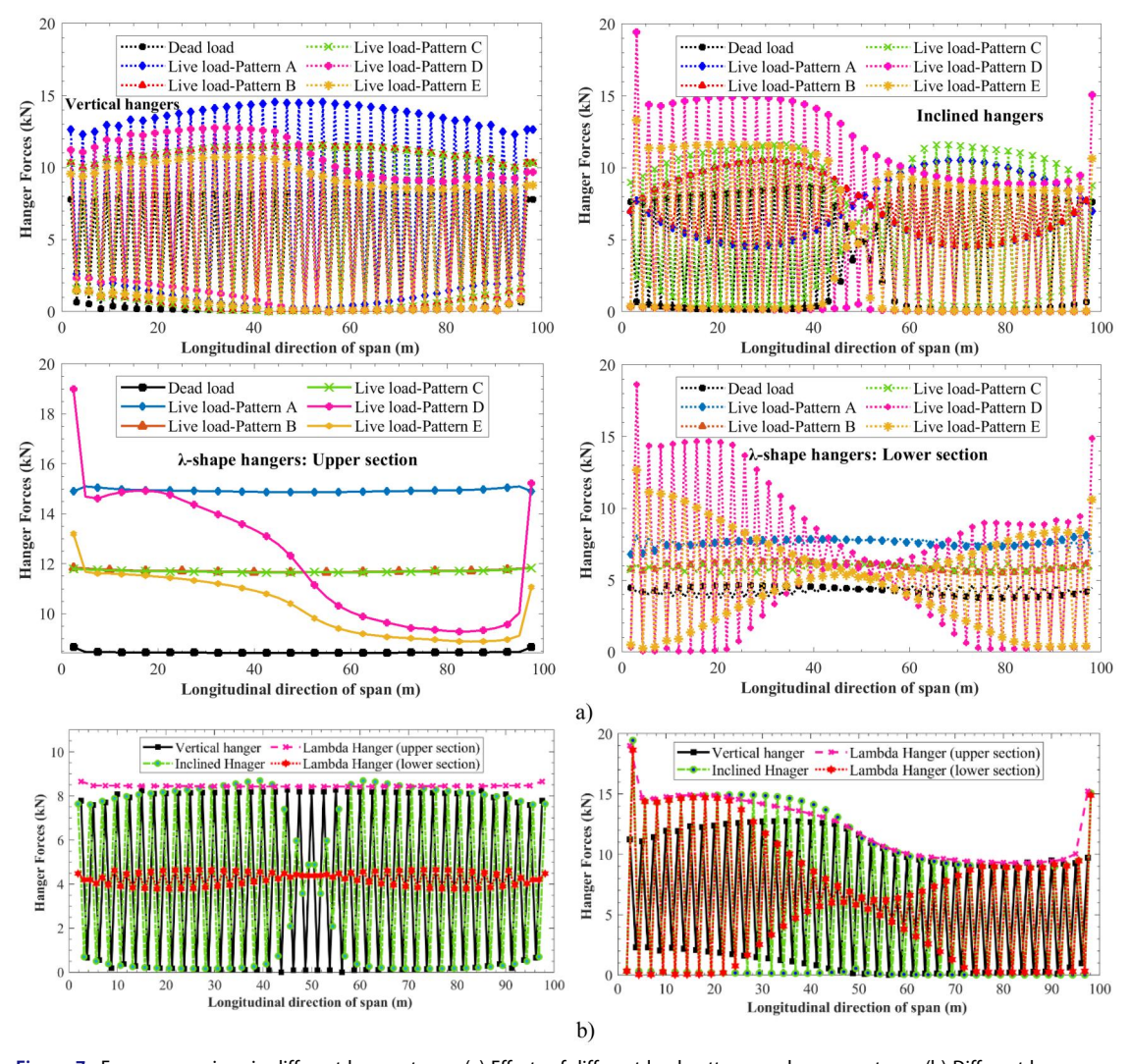


Figure 7. Force comparison in different hanger types. (a) Effects of different load patterns on hanger systems. (b) Different hangers under dead load (left), and live load pattern D (right).

Table 3. Force fluctuations of hangers due to live load.

Hanger type	Load Pattern	Α	В	С	D	E
Vertical	Max.	875%	121%	118%	773%	630%
	Min.	60%	-71%	-71%	-44%	-44%
Inclined	Max.	326%	178%	178%	829%	621%
	Min.	-9%	-9%	14%	-100%	-100%
λ-Shape (Upper section)	Max.	78%	39%	39%	120%	52%
	Min.	72%	37%	36%	10%	10%
λ -Shape (Lower section)	Max.	99%	48%	48%	344%	202%
•	Min.	52%	29%	28%	-99%	-94%

Table 4. Force distribution in different hanger systems due to applied load.

					Lambda-shaped hanger			
	Vertica	al hanger	Incline	d hanger	(Uppe	r Section)	(Lowe	r Section)
Load	Dead	Live (D)	Dead	Live (D)	Dead	Live (D)	Dead	Live (D)
Minimum Hanger Force (kN)	0.08	0.01	0.16	0	8.42	9.29	3.78	0
Maximum Hanger Force (kN)	8.28	12.76	8.69	19.43	8.66	19	4.65	18.64
Member Force Ratio (%)	99.03	100	98.17	100	2.73	51.12	18.75	100
Number of Slacked Hanger	0	7	0	37	0	0	0	28
Average force (kN)	4.19	5.95	4.32	6.14	8.45	12.2	4.26	6.14
Standard Deviation (kN)	3.97	5.19	3.78	6.36	8.42	4.19	8.42	4.19

than those in the lower section (4.3 kN). The maximum and minimum forces in the upper section are 8.66 and 8.42 kN (a 3% variation), while in the lower section, they are 3.78 and 4.65 kN (a 19% variation), respectively. Table 3 summarizes hanger force fluctuations under live loads, with most fluctuations for critical pattern D.

4.2.1. Comparing the lambda-shaped hanger system with conventional hangers

To compare the performance of vertical, inclined, and lambda-shaped hanger systems, a diagram of force distribution for the three systems is shown in Figure 7b. The analysis of force distribution in the lambda-shaped hanger system with vertical and inclined hangers under dead and live load is shown in Table 4. Under dead load, the ratio of minimum force to maximum force (force ratio) in the lambda-shaped hangers along the bridge is an average of 18.75% compared to the values of 99.03% and 98.17% for vertical and inclined hangers, respectively. The average force ratio in lambda-shaped hangers is 80% and 79% lower than the vertical and the inclined hangers, respectively. The most critical live load pattern that causes the most slackness in hangers is load pattern D. As a result, 7 vertical hangers, 37 inclined hangers, and 28 lambda-shaped hangers have slacked.

4.2.2. Effects of the hanger system on the response of the deck system

Load pattern D is the critical load pattern for the deck responses (Figure 8). Tensile force on the deck considering the inclined and lambda-shaped hangers is 19% and 24% lower than the deck with vertical hangers, respectively. The shear force considering vertical and lambda-shaped hangers is 10% and 2% more than that of inclined ones, respectively. Furthermore, the bending moment in the deck with lambda-shaped hangers is 0.56% lower than the case using inclined hangers. The hanger type and its load-transferring mechanism can affect the displacement of the deck. The maximum displacements of the deck considering different hanger systems under various load patterns are presented in Table 5. According to Figure 8 and Table 5, the maximum displacement for the vertical and inclined hanger systems are 481.84 and 380.94 mm, respectively, while it is 3.4% more in the lambda-shaped system.

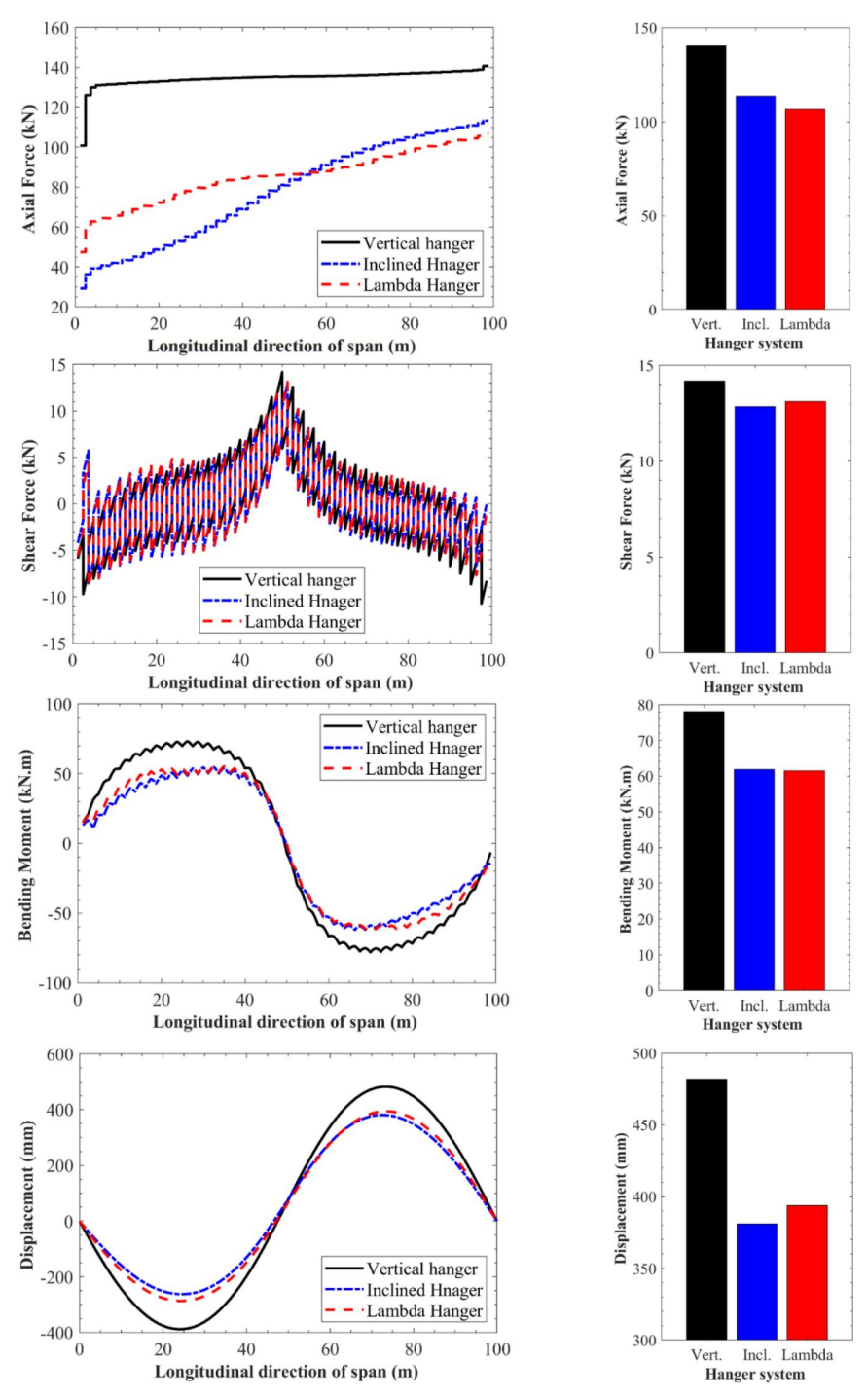


Figure 8. Force and displacement with their maximum values on the deck subjected to live load (Pattern D).

4.2.3. Effects of the hanger system on the responses of towers and main cables

Load pattern A causes maximum axial force in towers (Figure 9). With inclined hangers, the force is 757 kN. For lambda-shaped hangers, it's 0.33% lower. The load pattern D causes the highest

Table 5. Maximum vertical displacement (mm) stiffeners beam on deck due to different load patterns.

		Hanger Type				
Load	Pattern	Vertical	Inclined	Lambda-shaped		
Dead	_	78.9	64.59	79.29		
Live	Α	15.66	4.62	15.16		
	В	45.77	30.06	45.79		
	С	45.9	30.28	45.92		
	D	481.84	380.94	393.76		
	Ε	310.61	186.69	226.92		

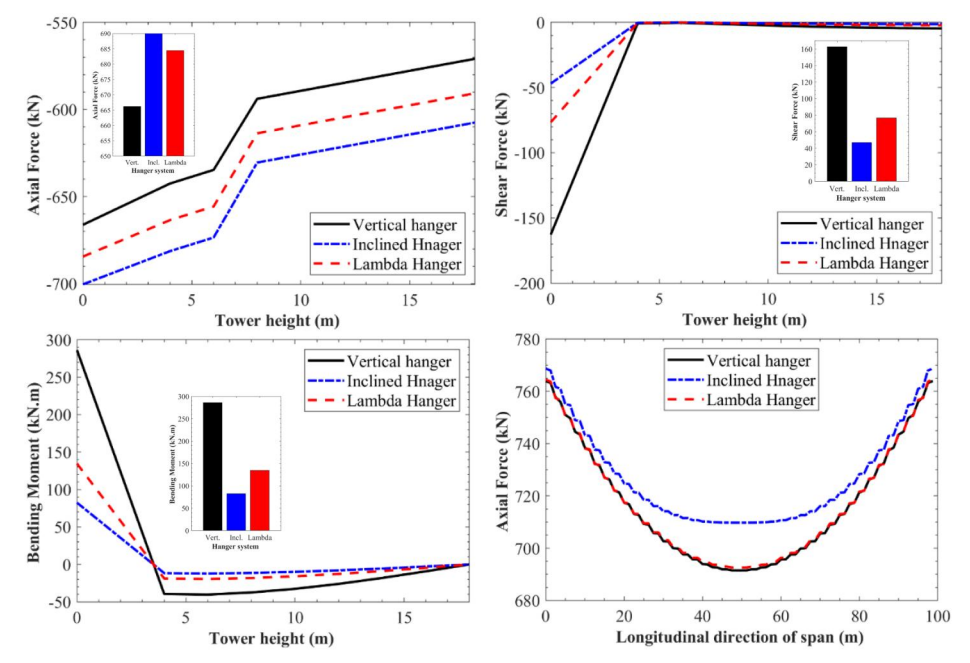
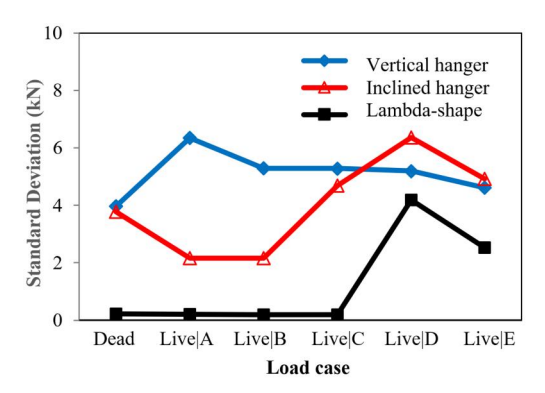


Figure 9. Forces in the tower and deck due to live load (Pattern A & D).

Table 6. Standard deviation of force in the hanger members due to different load patterns.

		Hanger Type			
Standard Deviation (kN)	Pattern	Vertical	Inclined	Lambda-shaped	
Dead Load	-	3.97	3.78	0.23	
Live Load	Α	6.34	2.16	0.21	
	В	5.29	2.16	0.2	
	С	5.28	4.69	0.19	
	D	5.19	6.36	4.19	
	Ε	4.61	4.92	2.53	

shear force in towers. The lambda-shaped hanger system's shear force is 63% higher than inclined hangers but 52.9% lower than vertical hangers. Although lambda-shaped shear force is higher than inclined, it's lower than vertical. The load pattern D also causes maximum bending moments. Bending moments with lambda-shaped hangers are 63.3% higher than inclined hangers but 53% lower than vertical hangers. Maximum axial force in the main cable occurs under load pattern A (Figure 9). Axial force is 763.9 kN for vertical hangers, 768.7 kN for inclined hangers, and 0.5% lower for lambda-shaped hangers compared to inclined ones.



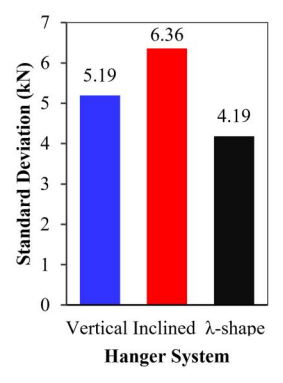


Figure 10. Standard deviation of axial force in hangers due to live load (Pattern *D*).

4.3. Comparing force distribution in hanger systems

By applying load to the suspension bridge, forces in hangers are generated. The force in each hanger is the function of the system's overall performance and the hangers' position along the bridge. A diffusion index should be used to investigate the force distribution in the hanger systems. One indicator of dispersion and distribution of data is the standard deviation. The standard deviation shows how much data are away from the median values. When the standard deviation is close to zero, the data are closer to the average. The values of the standard deviation for the force distribution in members of each hanger system are summarized in Table 6 considering different load patterns.

Figure 10 illustrates the performance comparison of the hanger systems under the most critical load pattern, *D*. In this pattern, the maximum force distribution is related to the inclined hanger system. Force distribution in members of lambda-shaped hangers is 34.1% lower than the case with the inclined hanger system. According to the results, the best case of force distribution is related to the lambda-shaped hanger system.

4.4. Optimum steel quantity

The optimized steel quantity for each type of hanger system is calculated. In comparison, the least amount of required steel is relating to the vertical hanger system $(0.292\,\text{kN})$. The amount of required steel for the inclined hanger system $(0.301\,\text{kN})$ is about 3% more than the vertical hanger system. However, the amount of required steel for the lambda-shaped hanger system $(0.302\,\text{kN})$ is about 0.33% more than inclined hangers.

4.5. Fatigue

The variation in traffic load over time induces fluctuations in the forces exerted on hangers, leading to stress variations that contribute to fatigue over prolonged cycles. This paper assesses the behavior of different hanger systems by examining the extent of force fluctuations as a key variable in fatigue development. Specifically, changes in live load directly impact the internal forces and, consequently, the stress experienced by hangers. These fluctuations in stress, arising from loading and unloading cycles, drive the fatigue phenomenon. Therefore, a hanger configuration capable of reducing fatigue effects from live load variations is essential. To evaluate the performance of the lambda-shaped hanger system relative to traditional configurations, we compared the force increment in each system under varied live-to-dead load ratios, as illustrated in Figure 11a. According to the different arrangements of hangers, force distribution in each system is varied compared to each other.

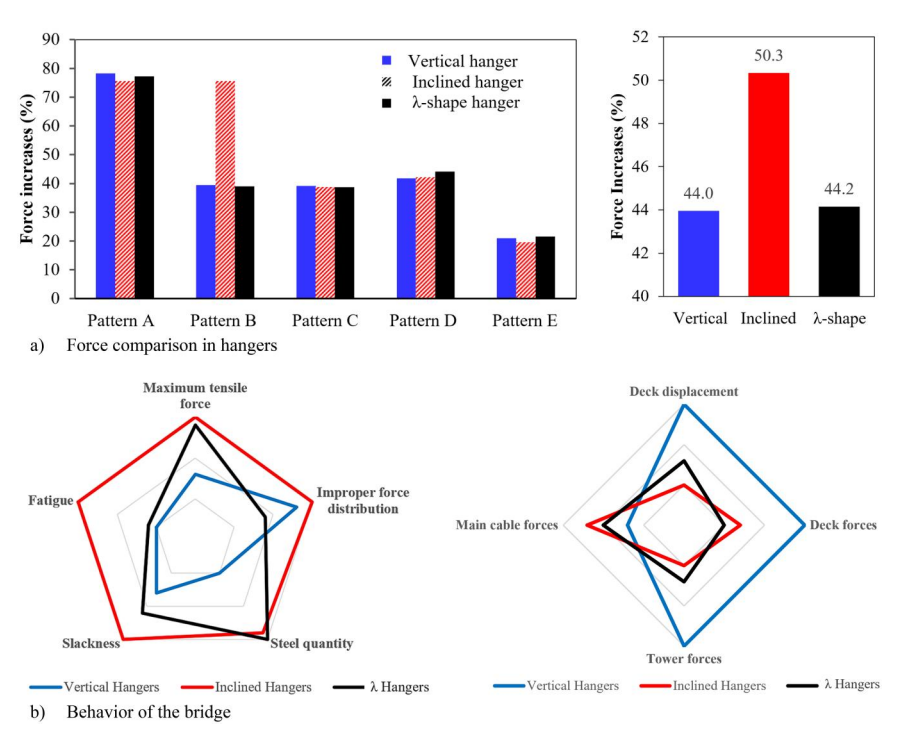


Figure 11. Performance evaluation considering different hanger systems. a) Force comparison in hangers. b) Behavior of the bridge.

Higher force increments through loading cycles in hangers due to varying load ratios increase fatigue vulnerability. Results show that the inclined hanger system exhibits the highest force increment by 50.3%, making it more susceptible to fatigue. The vertical hanger configuration exhibits a relatively lower fatigue vulnerability, with a force increment of 44%, indicating a more favorable performance regarding fatigue resistance. The lambda-shaped hangers achieve a force increment of 44.2%, closely matching vertical hangers and showing favorable fatigue performance. In comparison, the lambda-shaped configuration achieves a 3.9% lower force increment than inclined hangers, underscoring its advantage in fatigue resistance. Figure 11b further highlights force distribution in different members, with the lowest and most desirable values at the system center.

Compared with traditional vertical or inclined hangers, the lambda-shaped hanger system may require unique maintenance strategies due to its distinct geometry and force distribution characteristics. Engineers should focus particularly on inspecting connection points, as these play a critical role in maintaining structural integrity and preventing slackness. Additionally, regular checks for uniform stress distribution across the lambda-shaped hangers are essential to mitigate fatigue over time. Material durability and corrosion resistance should also be prioritized, as they directly affect the long-term performance of the hangers. Developing tailored inspection protocols can help ensure the system's effectiveness, especially in dynamic load conditions where force fluctuations may be more pronounced.

5. Conclusion

In this paper, a new hanger system called lambda-shaped hangers was introduced to improve the dynamic behavior of conventional hangers. The loading and unloading cycles over time cause

slackness and excessive tension in inclined hangers, and this process causes fatigue for the cable system. The effect of different variables (contributing to shear stiffness and damping characteristics) on the behavior of lambda-shaped hangers were investigated. The following results was obtained about the different hanger systems:

- The lambda-shaped hangers reduce the axial forces of inclined hangers and the slackness possibility, significantly due to efficient force distribution caused by their geometrical advantage. Therefore, the lambda-shaped hanger system exhibits improved performance against fatigue, comparable to that of vertical hangers, which are renowned for their excellent fatigue resistance in cable bridges.
- Similar to the bridge with vertical hangers, the maximum axial forces within the main cables of the bridge with lambda-shaped hangers became lower, compared to those of the bridge incorporating inclined hangers. This reduction is due to the ability of lambda-shaped hangers to distribute deck loads more evenly along the cable length, reducing peak stresses.
- Internal forces of the bridge deck in the case of lambda-shaped hangers became lower than inclined, and vertical hangers. Approximately, the same results were achieved for towers. The maximum vertical displacements of the deck with lambda-shaped hangers were reduced, compared to those with vertical hangers, although they were still slightly greater than those with inclined hangers. This improvement is due to the increased stiffness resulting from the angular configuration of the lambda-shaped hangers.
- The investigation revealed that pre-stressing is the most influential factor in reducing slackness in the lambda-shaped hanger system, as it provides effective stabilization under varying loads. The shape of the hangers also plays a significant role, contributing to both the reduction of slackness and the minimization of internal forces.

Considering the benefits, the lambda-shaped hangers can be the proper alternative to conventional hangers. Practical considerations for the lambda-shaped hanger system include factors such as connection detailing, optimum configuration, material durability, and ease of inspection and maintenance, which are likely to be critical to the system's long-term success in real-world applications. Future experimental research should focus on exploring the practical aspects of the lambda-shaped hanger system in more detail, including its structural performance under various environmental conditions and its long-term maintenance requirements.

Disclosure statement

The author(s) declared no potential conflicts of interest with respect to the research, authorship, and/or publication of this article.

Funding

The author(s) received no financial support for the research, authorship, and/or publication of this article.

ORCID

Arman Khatar (b) http://orcid.org/0009-0001-3384-9153 Salar Farahmand-Tabar (D) http://orcid.org/0000-0002-7520-5452 Majid Barghian (b) http://orcid.org/0000-0002-8765-7958

References

AASHTO GSDPB-2-I1. 2015. "Interim Revisions to LRFD Guide Specifications for the Design of Pedestrian Bridges." AASHTO 2015.



- Al-Khalili, M. A. 1984. "An Investigation into the Static Behaviour of the Existing Inclined Hanger System on the Severn Suspension Bridge." M.S. thesis, UMIST.
- Al-Smadi, Y. M., R. Z. Al-Rousan, A. A. Laradhi, and O. Avci. 2022. "Vibration Serviceability Investigation of a Curved Footbridge." Practice Periodical on Structural Design & Construction 27 (4): 04022040. https://doi.org/10. 1061/(ASCE)SC.1943-5576.0000714
- Avci, O. 2016. "Amplitude-Dependent Damping in Vibration Serviceability: Case of a Laboratory Footbridge." Journal of Archives of Engineering 22 (3): 04016005.
- Bachmann, H. 2002. "Lively Footbridges A Real Challenge." in: Proc. of Footbridge 2002. Design and Dynamic Behaviour of Footbridges, Paris, France.
- Barghian, M., and H. M. Faridani. 2011. "Proposing a New Model of Hangers in Pedestrian Suspension Bridges to Hangers Slackness Problem." Engineering 03 (04): 322-330. https://doi.org/10.4236/eng.2011.34037
- Bassoli, E., P. Gambarelli, and L. Vincenzi. 2018. "Human-Induced Vibrations of a Curved Cable-Stayed Footbridge." Journal of Constructional Steel Research 146: 84–96. https://doi.org/10.1016/j.jcsr.2018.02.001
- Brownjohn, J. M. W. 2005. Vibration serviceability of footbridges, IMACXXIII. USA: Orlando.
- BS5400. 2006. Part 2, Appendix C, Vibration serviceability requirements for foot and cycle track bridges. London: British Standards Institution.
- Carpineto, N., W. Lacarbonara, and F. Vestroni. 2010. "Mitigation of Pedestrian-Induced Vibrations in Suspension Footbridges via Multiple Tuned Mass Dampers." Journal of Vibration and Control 16 (5): 749-776. https://doi. org/10.1177/1077546309350188
- Dallard, P., A. J. Fitzpatrick, A. Flint, and S. Le Bourva. 2001. "Low A, Ridsdill Smith RM, Willford M. The London Millennium Footbridge." Struct. Eng 79 (22): 17-32.
- Dey, P., S. Narasimhan, and S. Walbridge. 2018. "Calibrating Pedestrian-Bridge Standards for Vibration Serviceability." Journal of Bridge Engineering 23 (10): 04018072. https://doi.org/10.1061/(ASCE)BE.1943-5592. 0001270
- Dey, P., S. Narasimhan, and S. Walbridge. 2021. "Reliability-Based Assessment and Calibration of Standards for the Lateral Vibration of Pedestrian Bridges." Engineering Structures 239: 112271. https://doi.org/10.1016/j.engstruct.2021.112271
- ENV 1995-2. 2005. "Eurocode 5, Design of Timber Structures Bridges." European Committee for Standardization
- Farahmand-Tabar, S., and M. Barghian. 2020a. "Formulating the Optimum Parameters of Modified Hanger System in the Cable-Arch Bridge to Restrain Force Fluctuation and Overstressing Problems." Journal of the Brazilian Society of Mechanical Sciences and Engineering 42 (9): 453. https://doi.org/10.1007/s40430-020-02513-0
- Farahmand-Tabar, S., and M. Barghian. 2020b. "Response Control of Cable-Stayed Arch Bridge Using Modified Hanger System." Journal of Vibration Control 26 (23-24): 2316-2328. https://doi.org/10.1177/1077546320921635
- Farahmand-Tabar, S., and M. Barghian. 2021. "Seismic Assessment of a Cable-Stayed Arch Bridge Under Three-Component Orthotropic Earthquake Excitation." Advanced Structural Engineering 24 (2): 227-242. https://doi. org/10.1177/1369433220948756
- Farahmand-Tabar, S., and M. Barghian. 2024. "Seismic Evaluation of the Bridge with a Hybrid System of Cable and Arch: Simultaneous Effect of Seismic Hazard Probabilities and Vertical Excitations." Mechanics Based Design of Structures and Machines 52 (4): 2136-2152. https://doi.org/10.1080/15397734.2023.2172029
- Farahmand-Tabar, S., M. Barghian, and M. Vahabzadeh. 2019. "Investigation of the Progressive Collapse in a Suspension Bridge Under the Explosive Load." International Journal of Steel Structures 19 (6): 2039-2050. https://doi.org/10.1007/s13296-019-00263-x
- Faravelli, L., and F. Ubertini. 2009. "Nonlinear State Observation for Cable Dynamics." Journal of Vibration and Control 15 (7): 1049-1077. https://doi.org/10.1177/1077546308094253
- Fib Bulletin 32. 2005. Guidelines for the design of footbridges. Fib Bulletin.
- Figueiredo, F. P., J. G. S. da Silva, L. R. O. de Lima, S. da, P. C. G. Vellasco, and S. A. L. de Andrade. 2008. "Parametric Study of Composite Footbridges under Pedestrian Walking Loads." Engineering Structures 30 (3): 605-615. https://doi.org/10.1016/j.engstruct.2007.04.021
- Gao, L., P. Wang, and Q. Ma. 2022. "Fatigue Performance of Steel Cables with Surface Defects." Composite Structures 279: 115393. https://doi.org/10.1016/j.compstruct.2022.115393
- García-Diéguez, M., V. Racic, and J. L. Zapico-Valle. 2021. "Complete Statistical Approach to Modelling Variable Pedestrian Forces Induced on Rigid Surfaces." Mechanical Systems and Signal Processing 159: 107800. https:// doi.org/10.1016/j.ymssp.2021.107800
- Hauksson, F. 2005. "Dynamic Behavior of Footbridges Pedestrian-Induced Vibrations." Master's Dissertation, Lund University.
- Huang, M. H., D. P. Thambiratnam, and N. J. Perera. 2005. "Vibration Characteristics of Shallow Suspension Bridge with Pre-Tensioned Cables." Engineering Structures 27 (8): 1220-1233. https://doi.org/10.1016/j.engstruct. 2005.03.005

- Kerr, S. C., and N. W. M. Bishop. 2001. "Human Induced Loading on Flexible Staircases." Engineering Structures 23 (1): 37–45. https://doi.org/10.1016/S0141-0296(00)00020-1
- Lai, E., C. Gentile, and M. G. Mulas. 2017. "Experimental and Numerical Serviceability Assessment of a Steel Suspension Footbridge." Journal of Constructional Steel Research 132: 16-28. https://doi.org/10.1016/j.jcsr.2017.
- Lepidi, M., V. Gattulli, and F. Vestroni. 2009. "Damage Identification in Elastic Suspended Cables through Frequency Measurement." Journal of Vibration and Control 15 (6): 867-896. https://doi.org/10.1177/ 1077546308096107
- Li, B., Y. L. Xie, and S. K. Au. 2022. "Measuring Configuration of Multi-Setup Ambient Vibration Test." Mechanical Systems and Signal Processing 175: 109153. https://doi.org/10.1016/j.ymssp.2022.109153
- Lievens, K., G. Lombaert, K. Van Nimmen, G. De Roeck, and P. Van den Broeck. 2018. "Robust Vibration Serviceability Assessment of Footbridges Subjected to Pedestrian Excitation: Strategy and Applications." Engineering Structures 171: 236-246. https://doi.org/10.1016/j.engstruct.2018.05.047
- Liu, B., Y. Wang, T. Rabczuk, T. Olofsson, and W. Lu. 2024. "Multi-Scale Modeling in Thermal Conductivity of Polyurethane Incorporated with Phase Change Materials Using Physics-Informed Neural Networks." Renewable Energy. 220: 119565. https://doi.org/10.1016/j.renene.2023.119565
- Mei, K., G. Jin, and S. Sun. 2018. "Nonlinear Vibrations of CFRP Cables Excited by Periodic Motions of Supports in Cable-Stayed Bridges." Journal of Vibration and Control 24 (22): 5249-5260. https://doi.org/10.1177/ 1077546317750503
- Melchor, B. C., P. H. Bouillard, E. Bodarwé, and L. Ney. 2004. "Structural Dynamic Design of a Footbridge under Pedestrian Loading." Struct and Mate Comput Mechanics Dept, Université Libre de Bruxelles, Av. F. D. Roosevelt 50, C.P. 194/5, 1050 Brussels (Belgium).
- Nakamura, S. 2003. "Field Measurements of Lateral Vibration on a Pedestrian Suspension Bridge." Structural Engineering 18: 22-26.
- Newland, D. E. 2003. "Vibration of London Millennium Bridge: Cause and Cure." International Journal of Acoustic Vibration 8 (1): 9-14. [Database][Mismatch
- Nyawako, D. S., and P. Reynolds. 2018. "Comparative Studies of Global and Targeted Control of Walkway Bridge Resonant Frequencies." Journal of Vibration and Control 24 (9): 1670-1686. https://doi.org/10.1177/ 1077546316667323
- Otavio, B., R. Filipe, C. E. M. Lopes, V. W. Diniz, and P. A. M. Brabo. 2022. "Probabilistic Vibration Performance Assessment of a Long-Span Steel Footbridge." Journal of Performance of Constructed Facilities 36 (1): 04021115.
- Pavic, A., M. Willford, P. Reynolds, and J. Wright. 2002. "Key Results of Modal Testing of the Millennium Bridge, London." In Proceedings of the International Conference on the Design and Dynamic Behaviour of Footbridges, Paris, France.
- Pellegrino, C., G. Cupani, and C. Modena. 2010. "The Effect of Fatigue on the Arrangement of Hangers in Tied Arch Bridges." Engineering Structures 32 (4): 1140-1147. https://doi.org/10.1016/j.engstruct.2009.12.040
- Pothula, Ashwini, Abhijit Gupta, and Guru R. Kathawate. 2012. "Kathawate GR. Fatigue Failure in Random Vibration and Accelerated Testing." Journal of Vibration and Control 18 (8): 1199-1206. https://doi.org/10.1177/
- Saber, H., F. S. Samani, and F. Pellicano. 2023. "Vibration Reduction of Footbridges Subjected to Walking, Running, and Jumping Pedestrian." Journal of Vibration and Control 29 (13-14): 3227-3240. https://doi.org/10. 1177/10775463221093107
- Seiler, C., O. Fischer, and P. Huber. 2002. "Semi-Active MR Dampers in TMD's for Vibration Control of Footbridges, Part 2: Numerical Analysis and Practical Realization." Proc. of Footbridge 2002-Design and Dynamic Behaviour of Footbridge, Paris, France.
- Shirgir, S., S. Farahmand-Tabar, and P. Aghabeigi. 2024. "Optimum Design of Real-Size Reinforced Concrete Bridge via Charged System Search Algorithm Trained by Nelder-Mead Simplex." Expert Systems with Applications 238 (A): 121815. https://doi.org/10.1016/j.eswa.2023.121815
- Shirgir, S., and S. Farahmand-Tabar. 2025. "An Enhanced Optimum Design of a Takagi-Sugeno-Kang Fuzzy Inference System for Seismic Response Prediction of Bridges." Expert Systems with Applications 266: 126096. https://doi.org/10.1016/j.eswa.2024.126096
- Studničková, M. 2004. "The Effect of Pedestrian Traffic on the Dynamic Behavior of Footbridges." Acta Polytechnica, Czech Technical University Publishing House 44 (2): 47-51.
- Suh, J., and S. P. Change. 2000. "Experimental Study on Fatigue Behaviour of Wire Ropes." International Journal of Fatigue 22 (4): 339–347. https://doi.org/10.1016/S0142-1123(00)00003-7
- Wang, D., C. Wu, Y. Zhang, and S. Li. 2019. "Study on Vertical Vibration Control of Long-Span Steel Footbridge with Tuned Mass Dampers under Pedestrian Excitation." Journal of Constructional Steel Research 154: 84-98. https://doi.org/10.1016/j.jcsr.2018.11.021



- Wang, L., S. Nagarajaiah, W. Shi, and Y. Zhou. 2021. "Semi-Active Control of Walking-Induced Vibrations in Bridges Using Adaptive Tuned Mass Damper considering Human-Structure-Interaction." Engineering Structures 244: 112743. https://doi.org/10.1016/j.engstruct.2021.112743
- Wu, Q., K. Takahashi, and S. Nakamura. 2003. "Non-Linear Vibrations of Cables considering Loosening." Journal of Sound and Vibration 261 (3): 385-402. https://doi.org/10.1016/S0022-460X(02)01090-8
- Wu, Q., K. Takahashi, and S. Nakamura. 2001. "The Effect of Loosening of Cables on Seismic Response of the Cable-Stayed Bridge." Riron Oyo Rikigaku Koenkai KoenRonbunshu J 50: 229-230.
- Živanović, Stana, Aleksandar Pavić, and Paul Reynolds. 2007. "Probability-Based Prediction of Multi-Mode Vibration Response to Walking Excitation." Engineering Structures 29 (6): 942-954. https://doi.org/10.1016/j.engstruct.2006.07.004
- Zivanovic, S'., A. Pavic, and P. Reynolds. 2005. "Vibration Serviceability of Footbridges under Human-Induced Excitation: A Literature Review." Journal of Sound Vibration 279 (1-2): 1-74.
- Zivanovic, S. 2008. "Vibration Serviceability of a Footbridge under Vertical Pedestrian Load." 11th Symposium on Structural Dynamics and Vibration Measurement. Dubendorf, Switzerland: Ziegler Consultants.
- Zhou, L., and S. Wan. 2022. "Vibration Control of Footbridges Based on Local Resonance Band Gaps." Journal of Structural Engineering 148 (9): 04022137. https://doi.org/10.1061/(ASCE)ST.1943-541X.0003454
- Zhu, F, et al. 2019. "Fatigue Sensitivity Analysis of Structures: A Comprehensive Study." Mechanics of Materials: 133:Article No. 103280.